

Supplementary Information

Insight into the mechanism of modulated syntheses:

In situ synchrotron diffraction studies on the formation of Zr-fumarate MOF

Gesa Zahn,* Philip Zerner,* Jann Lippke, Fabian L. Kempf, Sebastian Lilienthal, Christian
A. Schröder, Andreas M. Schneider, Peter Behrens

Institut für Anorganische Chemie, Leibniz Universität Hannover, Callinstr. 9, 30167
Hannover, Germany; also at the ZFM - Center for Solid-State Chemistry and New Materials,
Leibniz Universität Hannover

* These two authors contributed equally to this study

Contents

S1	<i>Data evaluation with the Avrami-Erofeev and Sharp-Hancock formalisms</i>	2
S1.1	<i>Variation of the modulator concentration in the water-based synthesis</i>	5
S1.2	<i>Variation of the temperature in the DMF-based synthesis</i>	7
S1.3	<i>Variation of the amount of modulator in the DMF-based synthesis</i>	10
S1.4	<i>Variation of the water content in the DMF-based synthesis</i>	12
S2	<i>Powder X-ray diffraction (PXRD) patterns</i>	14
	<i>Literature</i>	15

S1 Data evaluation with the Avrami-Erofeev and Sharp-Hancock formalisms

For a long time, the Avrami-Erofeev equation (equation S1)^[1,2,3,4] or its linearized equivalent, the Sharp-Hancock formalism (equation S2)^[5] have been preferred in publications dealing with the evaluation of kinetic data concerning the formation of a solid from a liquid or from another solid (e.g. glass crystallisation). This is also true for the porous solids, as, e.g., silicium-aluminium phosphates like SAPO-34^[6], gallium oxyfluorophosphates like ULM-3 and ULM-4^[7], layered manganese thioantimonates^[8] several MOFs or ZIFs,^[9,10,11,12] and also the Zr-based UiO-66 and its derivatives.^[13]

$$\alpha(t) = 1 - e^{-(k \cdot t)^{n_{AE}}} \quad (\text{S1})$$

$$\ln[-\ln(1 - \alpha)] = n_{AE} \cdot \ln(k) + n_{AE} \cdot \ln(t - t_0) \quad (\text{S2})$$

$\alpha(t)$: degree of crystallisation
 t : time
 k : overall rate constant
 n_{AE} : Avrami exponent

Concerning the crystallisation of layered manganese thioantimonates, Engelke *et al.* showed that two crystallisation mechanisms occur during the synthesis of $\text{Mn}_2\text{Sb}_2\text{S}_5 \cdot \text{DAP}$ (DAP=1,3-diaminopropane). With increasing temperature the mechanism changes from a phase-boundary-controlled reaction (Avrami exponent $n_{AE} \approx 1$ for $\alpha < 0.75$ at 130 °C) to a diffusion-controlled reaction (Avrami exponent $n_{AE} \approx 0.5$ for $\alpha > 0.75$ at 130 °C). Furthermore, the presence of two crystalline intermediates could be detected at lower temperatures. These are transformed to the final product after a short period of time in a temperature range of 105-130 °C. Ahnfeldt *et al.*^[9] investigated the kinetics of Al-MOFs like CAU-1 and CAU-1-(OH)₂ using conventional and microwave heating. In general, the reaction and induction times are shortened when the temperature is increased.^[14] Apart from the fact that the microwave heating resulted in increased synthesis rates and thus in smaller particles, the kinetic evaluation according to Avrami-Erofeev and Sharp-Hancock revealed different crystallisation mechanisms comparing the microwave heating with conventional heating. Whereas the microwave-heated reaction shows a diffusion-controlled mechanism (Avrami exponent $n_{AE} \approx 0.6-0.8$), the conventional heating rather led to a

phase-boundary-controlled reaction (Avrami exponent $n_{AE} \approx 1.0-1.1$). The activation energy was calculated to 131-136 kJ irrespective of the heat source.^[9]

A classical nucleation-growth kinetic was also found by Millange *et al.* in a time-resolved *in situ* diffraction study of HKUST-1.^[11] In the quite fast formation of HKUST-1, no induction time is detectable and the Avrami-Erofeev and Sharp-Hancock evaluation revealed that the reaction is controlled by the formation of new nucleation sites (Avrami exponent $n_{AE} \approx 1.5$). They further revealed that the crystallisation of MIL-53(Fe) occurs via a metastable intermediate, the lifetime of which can be prolonged by decreasing the reaction temperature.

Another MOF of the MIL family, Mn-MIL-100, does not show any intermediate formation. Instead, the kinetic results indicate a two-stage reaction process with two different reaction mechanisms. At the beginning of the reaction, the crystallisation is nucleation-controlled with the Avrami exponent $n_{AE} \approx 2$ but changes to $n_{AE} \approx 1$ as the reaction proceeds.^[12] Recently, Ragon *et al.* investigated the crystallisation behaviour of the Zr-MOF UiO-66 and found out that the addition of both water and hydrochloric acid leads to faster crystallisation rates.^[13] Since they discovered that only the presence of water seems to be the cause for this acceleration, these results are in good agreement with this work and our previous observations.^[15]

Although the traditional Avrami-Erofeev-based mode of evaluation is well-established, the procedure proposed by Gualtieri in 2001 is becoming more and more popular. Millange *et al.* used this evaluation and pointed out that the Avrami-Erofeev method shows severe limitation since it had been developed for a specific solid-solid reaction. They emphasise that the fitting parameters are not applicable for heterogeneous crystallisation of a solid from a liquid. For that reason, the Gualtieri evaluation was applied for the investigation of the crystallisation of MOF-14. It was discovered that this reaction is nucleation rate-determined, because the calculated values for k_N were in all cases smaller than k_G .^[16]

A combined evaluation using Avrami-Erofeev and Sharp-Hancock as well as the Gualtieri model was applied by Cravillon *et al.*^[10] In this work the formate-modulated synthesis of ZIF-8 was investigated by using time-resolved *in situ* X-ray diffraction. On the one hand, the results of the Avrami-Erofeev and Sharp-Hancock evaluation revealed that the modulated synthesis of ZIF-8 is rate-limited by a phase-boundary reaction (Avrami exponent $n_{AE} \approx 1.0-1.3$). On the other hand, by applying the Gualtieri evaluation, k_N was in all cases smaller than k_G , so that the calculations resulted in a nucleation-controlled

reaction rate. This work illustrates the divergence of the different models and demands a sensitive judgement concerning the evaluation of kinetic data on the formation of a solid.

Given the uncertainties in the interpretation of kinetic data obtained with the Avrami-based evaluation, especially with regard to the meaning of different Avrami exponents n_{AE} ^[17] and to the fact that this equation was originally compiled for the description of a solid-solid crystallisation,^[1,2,3] we preferred to present our results as obtained by the evaluation using the Gualtieri equation.^[18] The fact that this equation contains two different terms for nucleation and crystal growth fits well to the investigated reactions. In fact, it allows us in some cases to obtain a deeper interpretation of the kinetic data, for example when it is found that the activation energies for nucleation and growth are very similar, indicating that the same basic process is concerned in the corresponding rate-determining steps.

In contrast, the evaluation methods according to Avrami-Erofeev as well as to Sharp and Hancock (effectively a linearization of the Avrami-Erofeev equation) do not contain separate terms for the nucleation and growth. However, in order to be able to compare our kinetic investigations to studies of MOF formation reactions where the data were evaluated by applying the Avrami-Erofeev and Sharp-Hancock equations, we here present the results of the analysis of our data when these formalisms are used.

S1.1 Variation of the modulator concentration in the water-based synthesis

water, 43 °C, x eq modulator

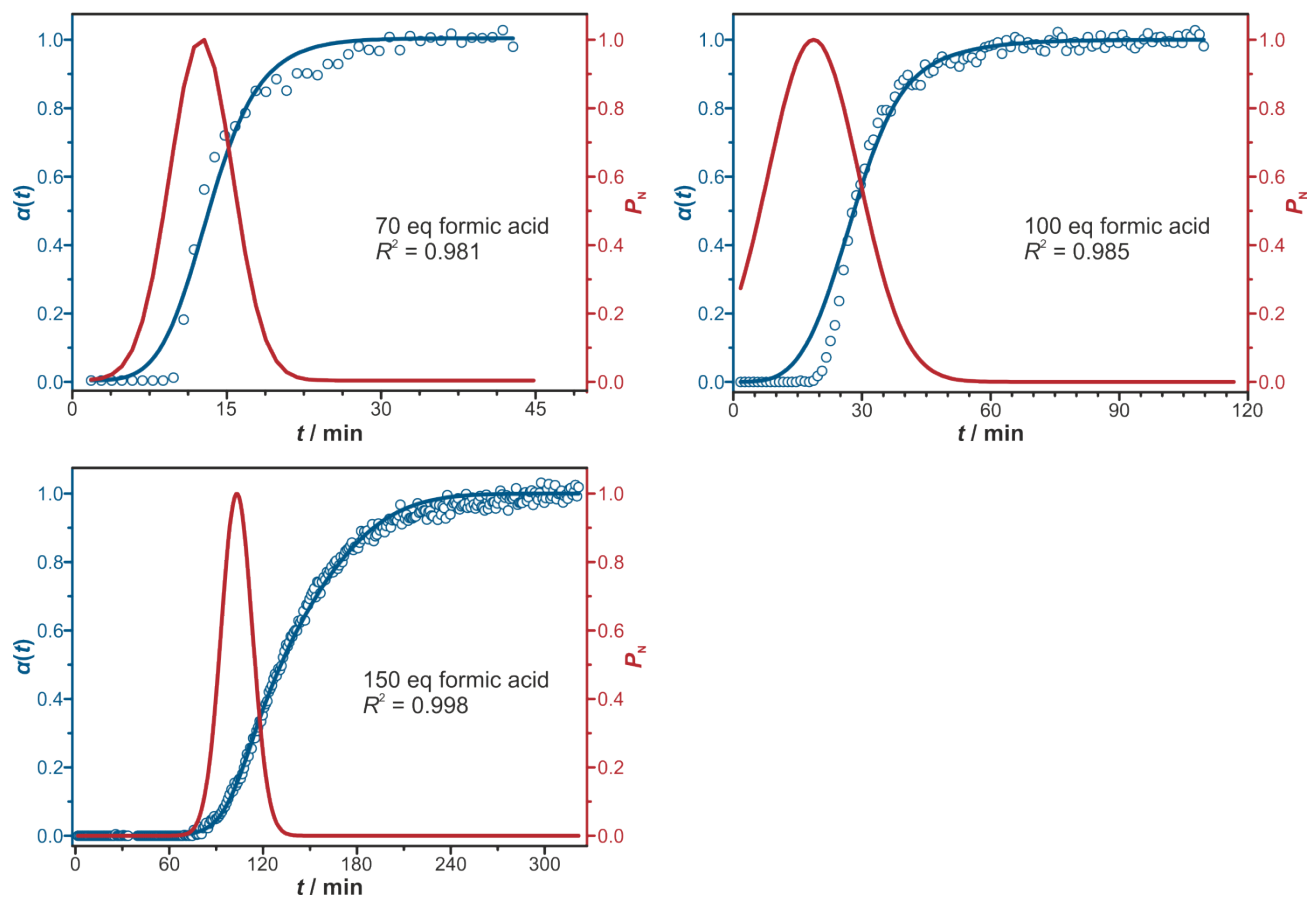


Figure S1. Extent of crystallisation α plotted against time t (blue circles) and the corresponding Gaultieri fitting (blue curve) as well as the probability for nucleation P_N (red curve) for varied amounts of modulator in water. The reactions studied here were carried out at 43 °C with molar ratios $ZrCl_4/H_2fum/formic\ acid/H_2O$ of 1:3:x:1074.

water, 43 °C, x eq modulator

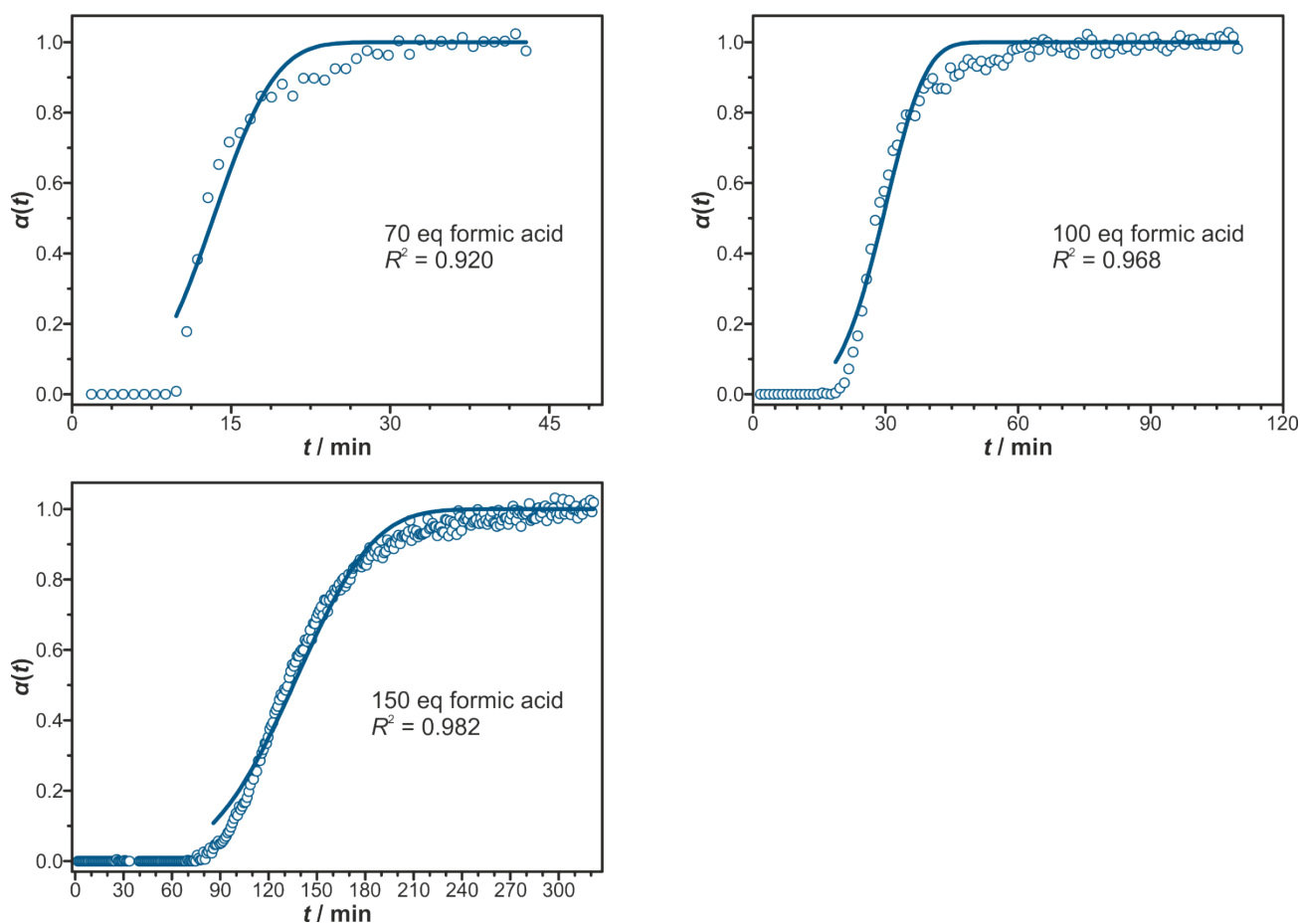


Figure S2. Extent of crystallisation α plotted against time t (blue circles) and the corresponding Avrami-Erofeev fitting (blue curve) for varied amounts of modulator in water. The reactions studied here were carried out at 43 °C with molar ratios $\text{ZrCl}_4/\text{H}_2\text{fum}/\text{formic acid}/\text{H}_2\text{O}$ of 1:3:x:1074.

water, 43 °C, x eq modulator

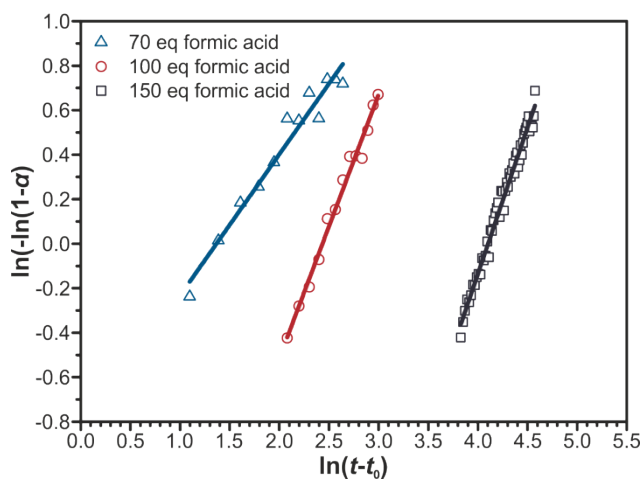


Figure S3. Sharp-Hancock plots for varied amounts of modulator in water. The reactions studied here were carried out at 43 °C with molar ratios $\text{ZrCl}_4/\text{H}_2\text{fum}/\text{formic acid}/\text{H}_2\text{O}$ of 1:3:x:1074.

Table S1. Kinetic parameters obtained by fitting of the crystallisation curves with the Avrami-Erofeev and Sharp-Hancock equation. Crystallisation curves were measured for syntheses of Zr-*fum* MOF in water-based systems under variation of the concentration (x equivalents) of the modulator formic acid (ZrCl₄/H₂*fum*/formic acid/water 1:3: x :1074, 43 °C).

x	n_{AE}	k_{AE} / min^{-1}	n_{SH}	k_{SH} / min^{-1}
70	3.3(4)	0.067(1)	0.79(5)	0.242(1)
100	4.4(2)	0.031(1)	1.40(5)	0.088(1)
150	3.9(1)	0.007(1)	1.45(1)	0.017(1)

S1.2 Variation of the temperature in the DMF-based synthesis

DMF, x °C, 70 eq modulator

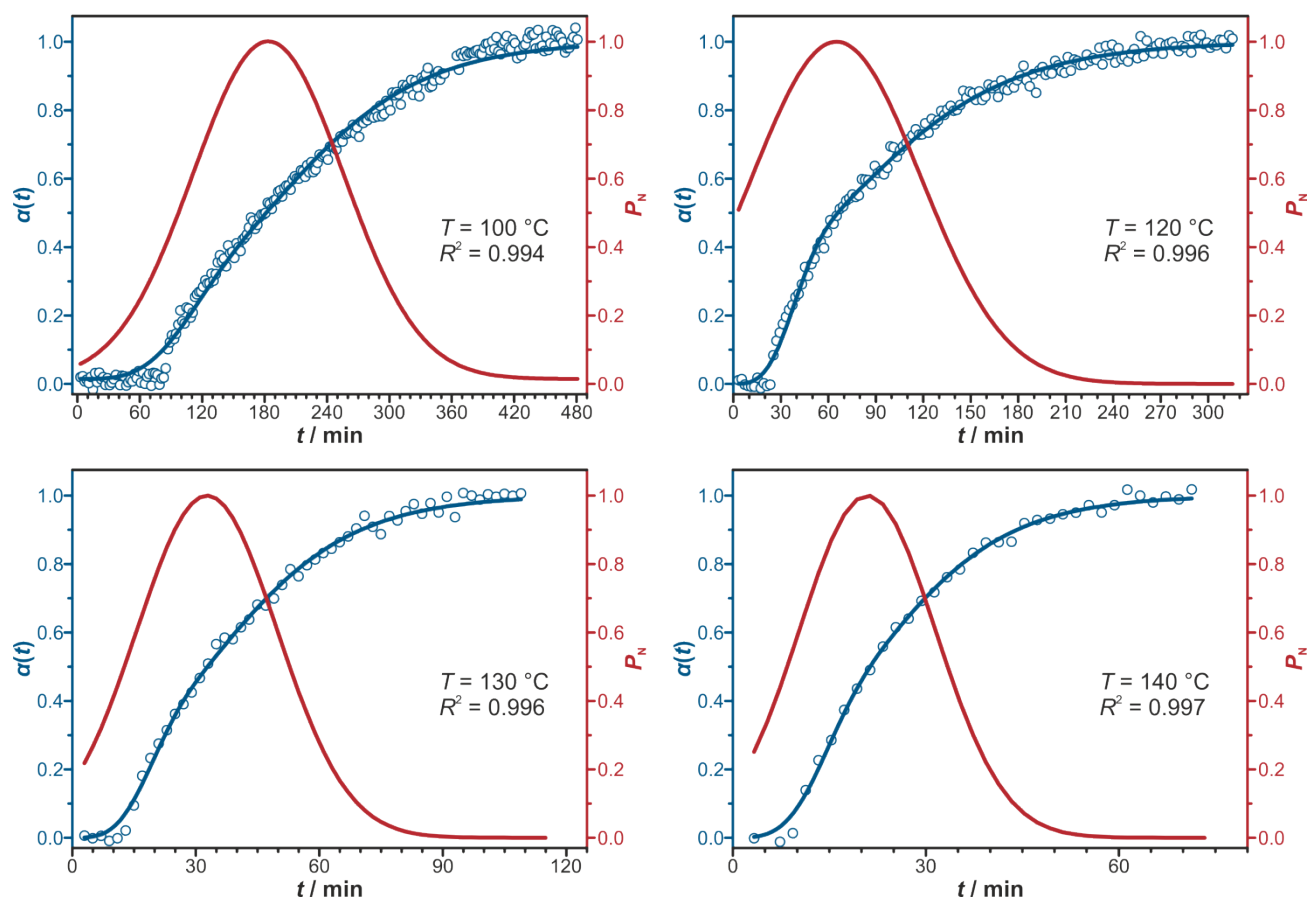


Figure S4. Extent of crystallisation α plotted against time t (blue circles) and the corresponding Guiltieri fitting (blue curve) as well as the probability for nucleation P_N (red curve) for varied temperatures. The reactions studied here were carried out in DMF with molar ratios ZrCl₄/H₂*fum*/formic acid/DMF of 1:3:70:500.

DMF, x °C, 70 eq modulator

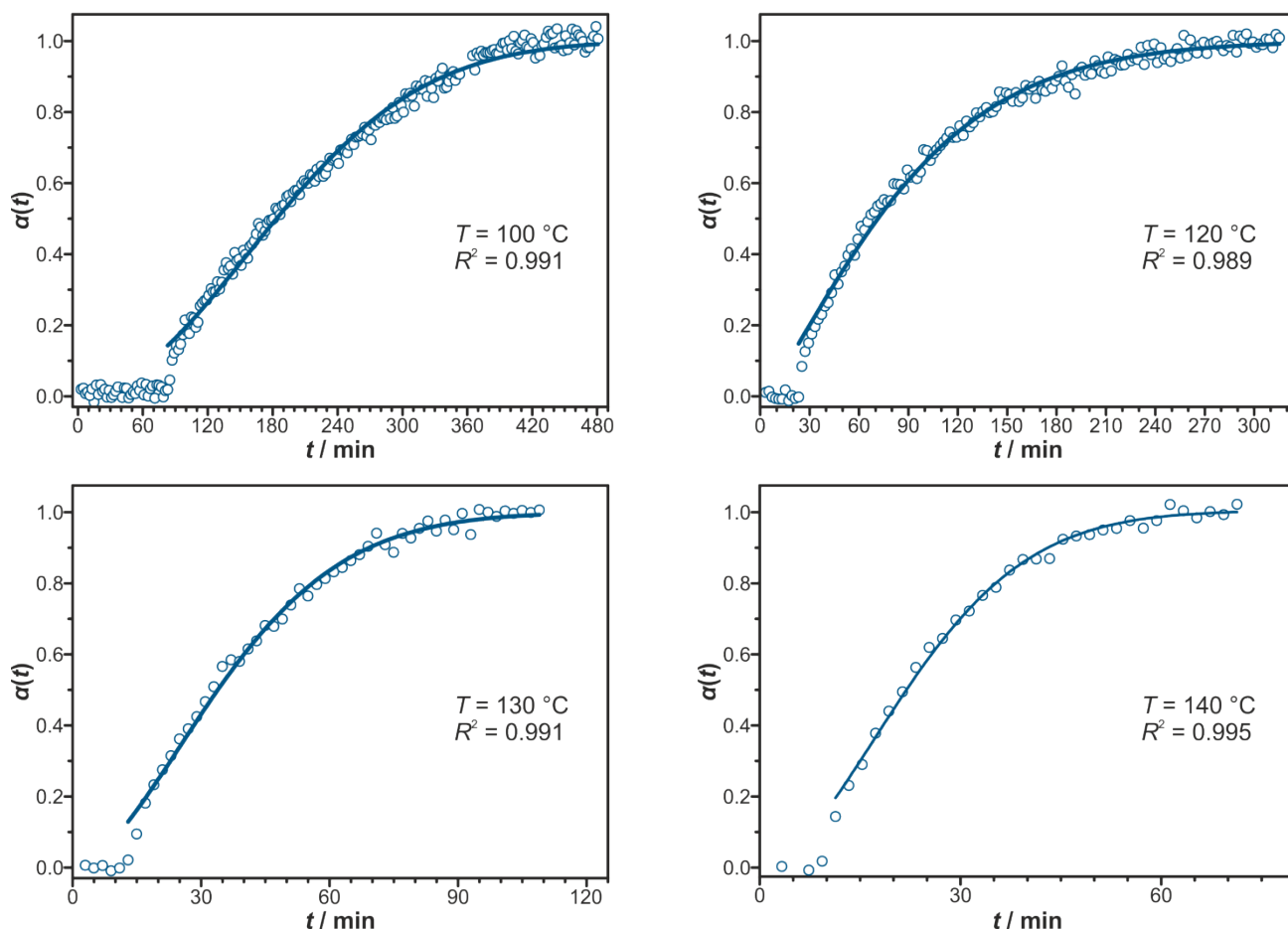


Figure S5. Extent of crystallisation α plotted against time t (blue circles) and the corresponding Avrami-Erofeev fitting (blue curve) for varied temperatures. The reactions studied here were carried out in DMF with molar ratios $\text{ZrCl}_4/\text{H}_2\text{fum}/\text{formic acid}/\text{DMF}$ of 1:3:70:500.

DMF, x °C, 70 eq modulator

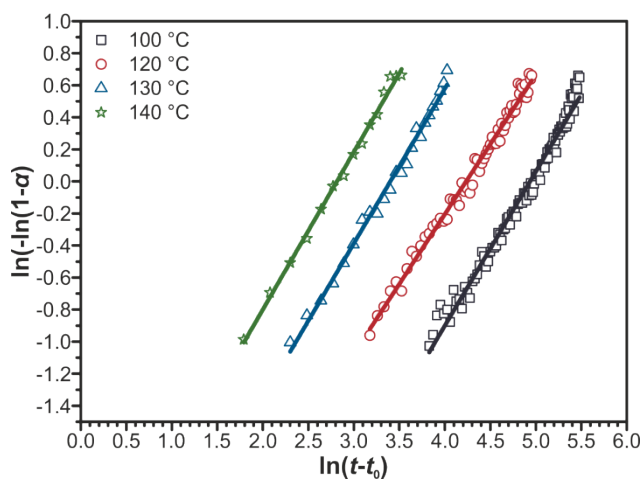


Figure S6. Sharp-Hancock plots for varied temperatures. The reactions studied here were carried out in DMF with molar ratios $\text{ZrCl}_4/\text{H}_2\text{fum}/\text{formic acid}/\text{DMF}$ of 1:3:70:500.

Table S2. Kinetic parameters obtained by fitting of the crystallisation curves with the Avrami-Erofeev and Sharp-Hancock equation. Crystallisation curves were measured for syntheses of Zr-*fum* MOF in DMF-based systems under variation of the temperature T (ZrCl₄/H₂*fum*/formic acid /DMF 1:3:70:500).

$T / ^\circ\text{C}$	n_{AE}	$k_{\text{AE}} / \text{min}^{-1}$	n_{SH}	$k_{\text{SH}} / \text{min}^{-1}$
100	1.99(2)	0.0045(1)	1.04(2)	0.0075(1)
120	1.30(2)	0.0106(1)	0.88(1)	0.0150(1)
130	1.68(4)	0.0237(2)	1.03(2)	0.0361(1)
140	1.77(4)	0.0368(3)	1.06(2)	0.0590(1)

Table S3. Activation energies obtained from the Arrhenius evaluation of temperature-variable rate constants as obtained by applying the Avrami-Erofeev and the Sharp-Hancock fitting.

<i>Avrami-Erofeev</i>	<i>Sharp-Hancock</i>
$E_{\text{A}} / \text{kJ}\cdot\text{mol}^{-1}$	$E_{\text{A}} / \text{kJ}\cdot\text{mol}^{-1}$
69 ± 7	67 ± 10

S1.3 Variation of the amount of modulator in the DMF-based synthesis

DMF, 120 °C, x eq modulator

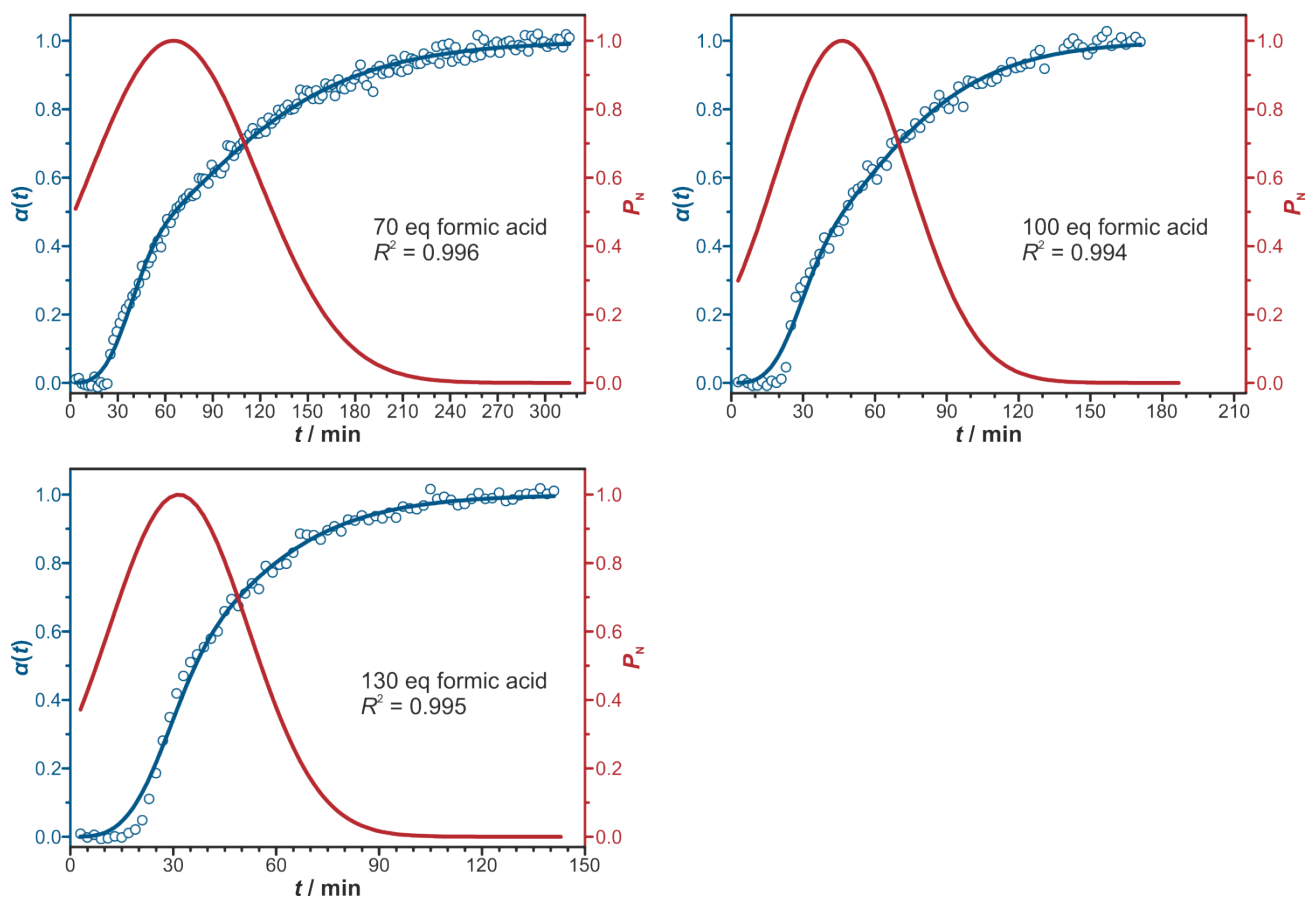


Figure S7. Extent of crystallisation α plotted against time t (blue circles) and the corresponding Gualtieri fitting (blue curve) as well as the probability for nucleation P_N (red curve) for varied amounts of modulator in DMF. The reactions studied here were carried out at 120 °C with molar ratios $ZrCl_4/H_2fum/formic\ acid/DMF$ of 1:3:x:500.

DMF, 120 °C, x eq modulator

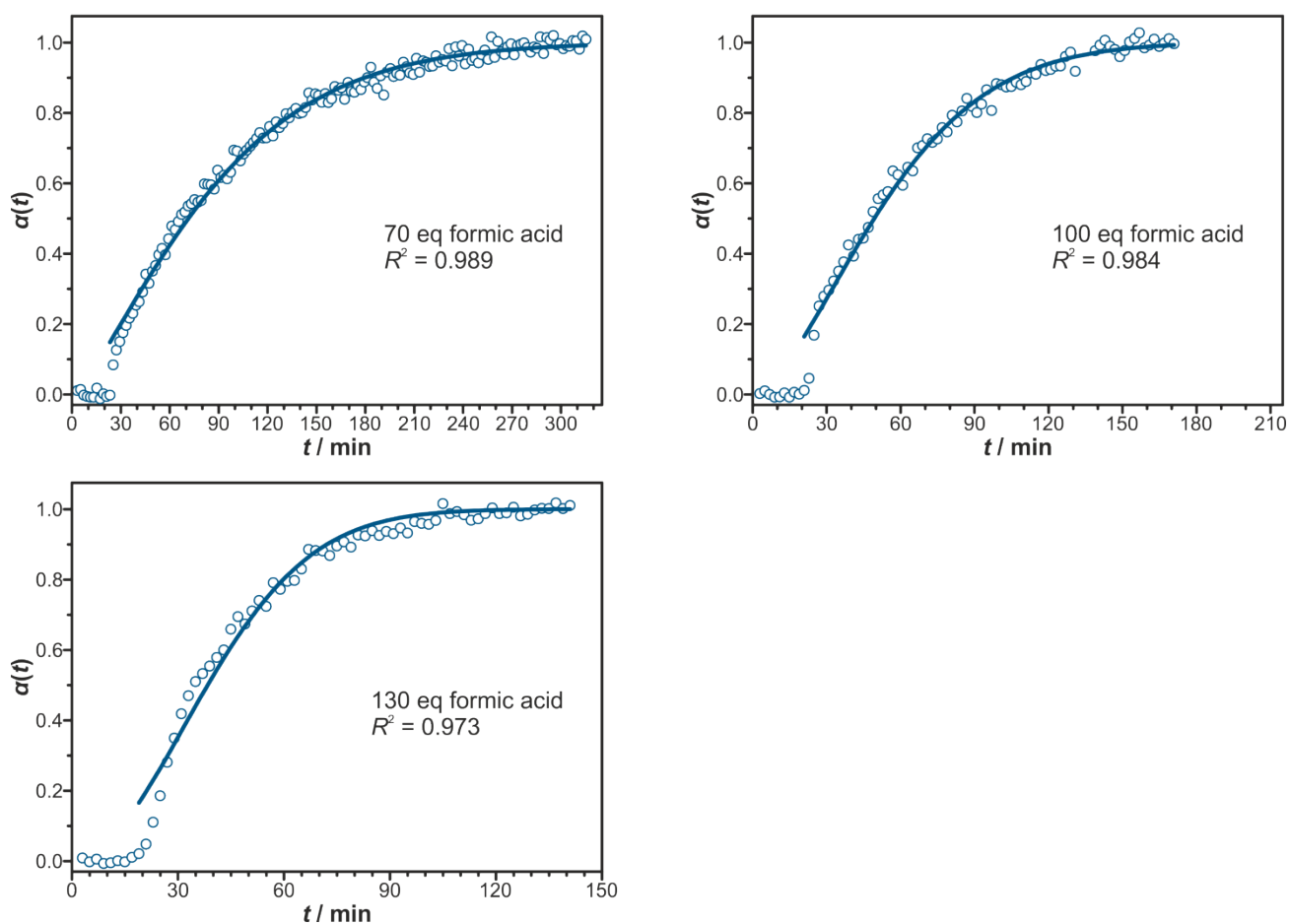


Figure S8. Extent of crystallisation α plotted against time t (blue circles) and the corresponding Avrami-Erofeev fitting (blue curve) for varied amounts of modulator in DMF. The reactions studied here were carried out at 120 °C with molar ratios $ZrCl_4/H_2fum/formic\ acid/DMF$ of 1:3:x:500.

DMF, 120 °C, x eq modulator

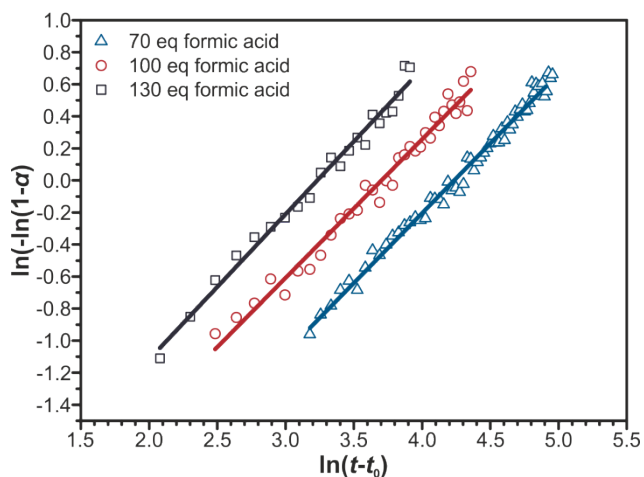


Figure S9. Sharp-Hancock plots for varied amounts of modulator in DMF. The reactions studied here were carried out at 120 °C with molar ratios $ZrCl_4/H_2fum/formic\ acid/DMF$ of 1:3:x:500.

Table S4. Kinetic parameters obtained by fitting of the crystallisation curves with the Avrami-Erofeev and Sharp-Hancock equation. Crystallisation curves were measured for syntheses of Zr-*fum* MOF in DMF-based systems under variation of the concentration (x equivalents) of the modulator formic acid (ZrCl₄/H₂*fum*/formic acid /DMF 1:3: x :500, 120 °C).

x	n_{AE}	k_{AE} / min^{-1}	n_{SH}	k_{SH} / min^{-1}
70	1.30(2)	0.0106(1)	0.88(1)	0.0150(1)
100	1.57(4)	0.0161(2)	0.90(2)	0.0259(1)
130	1.90(8)	0.0215(3)	0.93(3)	0.0407(1)

S1.4 Variation of the water content in the DMF-based synthesis

DMF, 100 °C, 70 eq modulator, x eq water

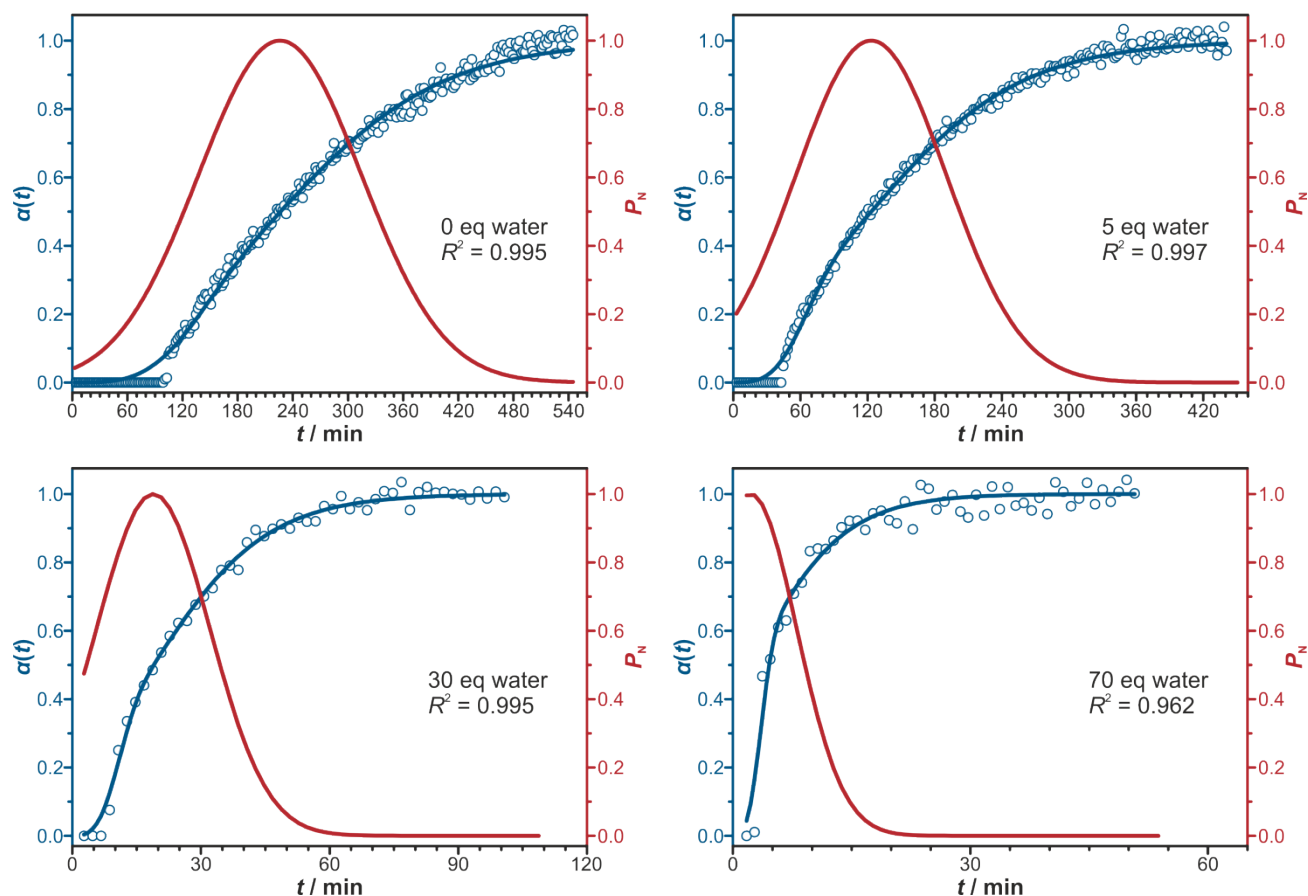


Figure S10. Extent of crystallisation α plotted against time t (blue circles) and the corresponding Guiltieri fitting (blue curve) as well as the probability for nucleation P_N (red curve) for varied amounts of water in DMF. The reactions studied here were carried out at 100 °C with molar ratios ZrCl₄/H₂*fum*/formic acid/water/DMF of 1:3:70: x :500.

DMF, 100 °C, 70 eq modulator, x eq water

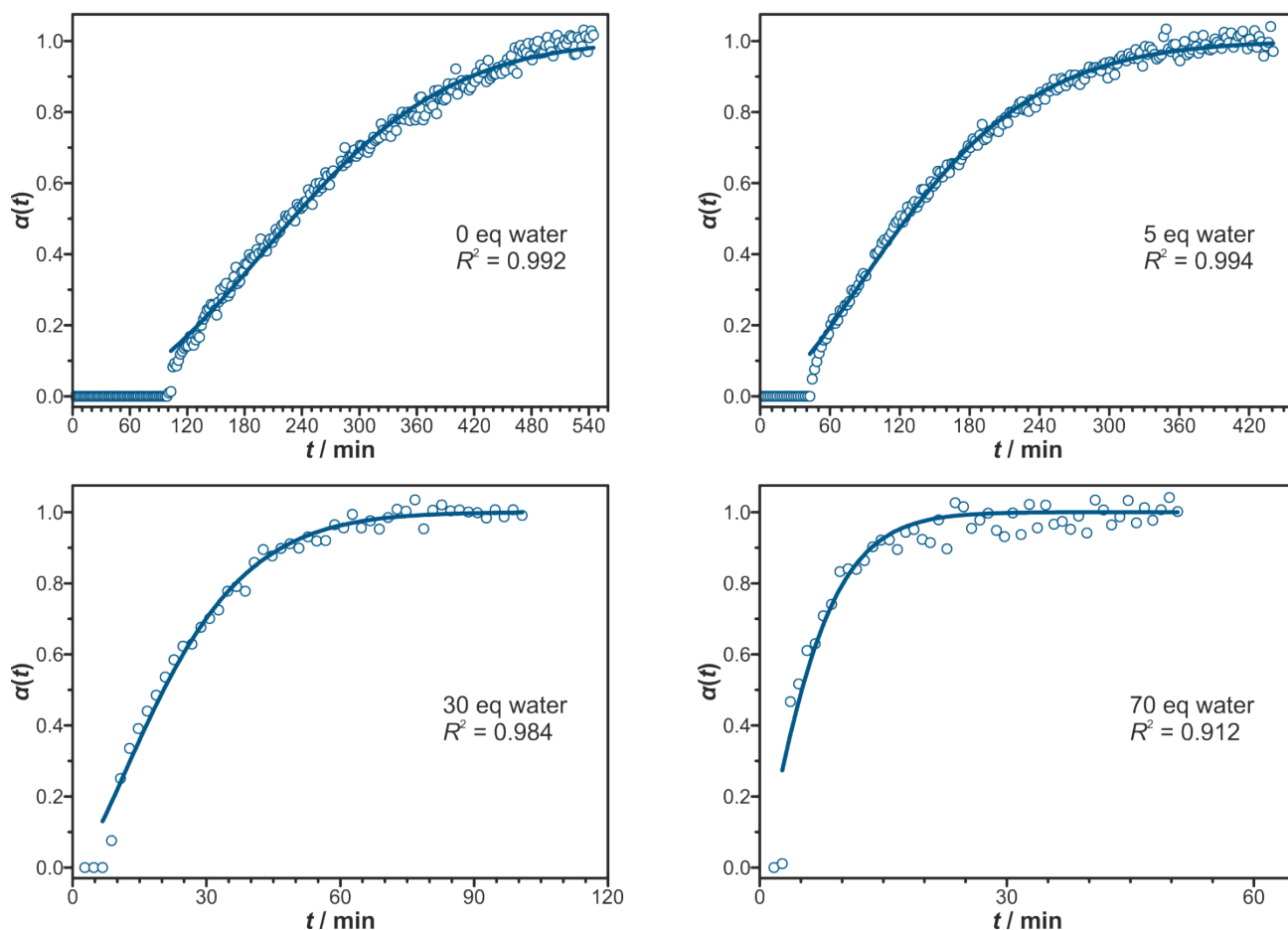


Figure S11. Extent of crystallisation α plotted against time t (blue circles) and the corresponding Avrami-Erofeev fitting (blue curve) for varied amounts of water in DMF. The reactions studied here were carried out at 100 °C with molar ratios $ZrCl_4/H_2fum/formic\ acid/water/DMF$ of 1:3:70:x:500.

DMF, 100 °C, 70 eq modulator, x eq water

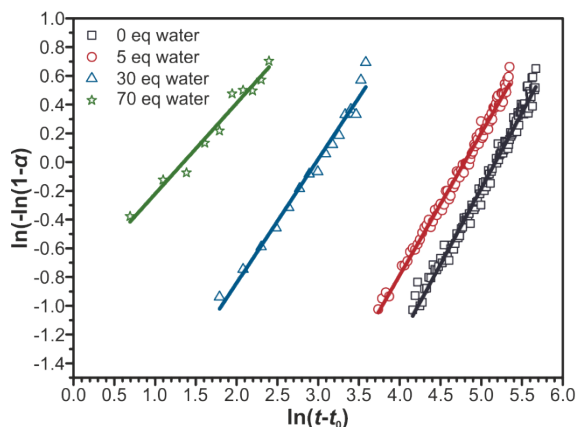


Figure S12. Sharp-Hancock plots for varied amounts of water in DMF. The reactions studied here were carried out at 100 °C with molar ratios $ZrCl_4/H_2fum/formic\ acid/water/DMF$ of 1:3:70:x:500.

Table S5. Kinetic parameters obtained by fitting of the crystallisation curves with the Avrami-Erofeev and Sharp-Hancock equation. Crystallisation curves were measured for syntheses of *Zr-fum* MOF in DMF-based systems under variation of the concentration (x equivalents) of water ($\text{ZrCl}_4/\text{H}_2\text{fum}/\text{formic acid}/\text{water}/\text{DMF}$ 1:3:70: x :500, 100 °C).

x	n_{AE}	$k_{\text{AE}} / \text{min}^{-1}$	n_{SH}	$k_{\text{SH}} / \text{min}^{-1}$
0	2.02(2)	0.0036(1)	1.09(1)	0.0060(1)
5	1.57(2)	0.0063(1)	1.01(1)	0.0089(1)
30	1.44(5)	0.0380(6)	0.84(2)	0.0541(1)
70	1.2(1)	0.145(5)	0.68(4)	0.2893(1)

S2 Powder X-ray diffraction (PXRD) patterns

Powder X-ray diffraction (PXRD) patterns were measured on the products after the reactions using a Stoe StadiP diffractometer working in transmission mode and operated with Ge(111)-monochromatized $\text{CuK}_{\alpha 1}$ radiation ($\lambda = 1.54060 \text{ \AA}$). An exemplary PXRD pattern of a *Zr-fum* MOF sample that was collected after the reaction is shown in Figure S13.

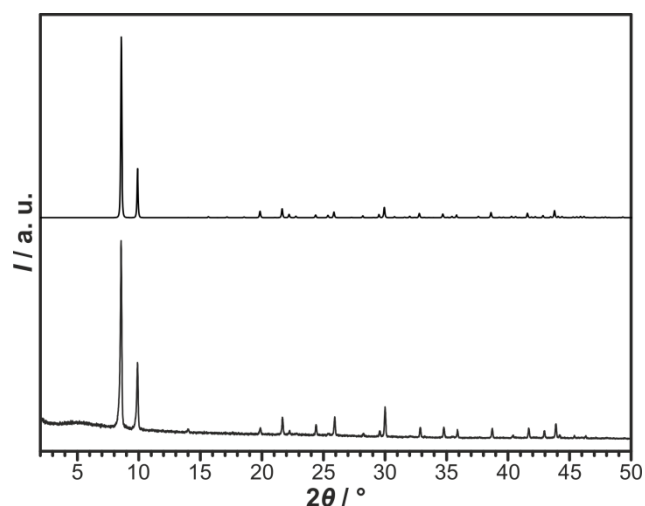


Figure S13. Simulated PXRD pattern for the *Zr-fum* MOF¹⁵ (top) and PXRD pattern of a *Zr-fum* MOF sample after the reaction during which its formation was studied (bottom, molar ratios $\text{ZrCl}_4/\text{H}_2\text{fum}/\text{formic acid}/\text{H}_2\text{O}$ of 1:3:150:1074 at 43 °C).

Literature

- 1 M. Avrami, *J. Chem. Phys.*, 1939, **7**, 1103.
- 2 M. Avrami, *J. Chem. Phys.*, 1940, **8**, 212.
- 3 M. Avrami, *J. Chem. Phys.*, 1941, **9**, 177.
- 4 The original Avrami-Erofeev equation was formulated as $\alpha(t) = 1 - e^{-k \cdot t^n}$, i.e. without brackets around the term $-k \cdot t$. However, in today's application, the form given as in equation S1 is preferred. Therefore, for better comparison, this form of the equation is also used here. The original formulation was given by Erofeev (B. V. Erofeev, *Dokl. Akad. Nauk SSSR*, 1946, **52**, 511, cited after ref. 17, supporting information). In addition, Khanna and Taylor found that only the modified equation provides meaningful data on reaction rates and activation energies (Y. P. Khanna and T. J. Taylor, *Polym. Eng. Sci.*, 1988, **28**, 1042).
- 5 J. D. Hancock and J.H. Sharp, *J. Am. Ceram. Soc.*, 1972, **55**, 74.
- 6 Ø. B. Vistad, D. E. Akporiaye and K. P. Lillerud, *J. Phys. Chem. B*, 2001, **105**, 12437.
- 7 R. I. Walton, T. Loiseau, D. O'Hare and G. Férey, *Chem. Mater.*, 1999, **11**, 3201.
- 8 L. Engelke, M. Schaefer, M. Schnur and W. Bensch, *Chem. Mater.*, 2001, **13**, 1383.
- 9 T. Ahnfeldt, J. Moellmer, V. Guillerm, R. Staudt, C. Serre and N. Stock, *Chem. Eur. J.*, 2011, **17**, 6462.
- 10 J. Cravillon, C. A. Schröder, H. Bux, A. Rothkirch, J. Caro and M. Wiebcke, *CrystEngComm*, 2012, **14**, 492.
- 11 F. Millange, M. I. Medina, N. Guillou, G. Férey, K. M. Golden, R. I. Walton and *Angew. Chem. Int. Ed.*, 2010, **49**, 763.
- 12 H. Reinsch and N. Stock, *CrystEngComm*, 2013, **15**, 544.
- 13 F. Ragon, P. Horcajada, H. Chevreau, Y. K. Hwang, U. Lee, S. R. Miller, T. Devic, J. Chang and C. Serre, *Inorg. Chem.*, 2014, **53**, 2491.
- 14 P. Norby and J. C. Hanson, *Catal. Today*, 1998, **39**, 301.
- 15 G. Wißmann, A. Schaate, S. Lilienthal, I. Bremer, A. M. Schneider and P. Behrens, *Microporous Mesoporous Mater.*, 2012, **152**, 64.

- 16 F. Millange, R. El Osta, M. E. Medina and R. I. Walton, *CrystEngComm*, 2011, **13**, 103.
- 17 E. E. Finney and R. G. Finke, *Chem. Mater.*, 2009, **21**, 4692.
- 18 A. F. Gualtieri, *Phys. Chem. Miner.*, 2001, **2**, 719.